JOURNAL OF MOLECULAR SPECTROSCOPY 67, 157–184 (1977)

An Analysis of the O_2^+ $b^4\Sigma_g^-$–$a^4\Pi_u$ First Negative Band System

D. L. ALBRITTON, A. L. SCHMELTEKOPF, AND W. J. HARROP

Aeronomy Laboratory, NOAA Environmental Research Laboratories, Boulder, Colorado 80302

R. N. ZARE

Department of Chemistry, Columbia University, New York, New York 10027

AND

J. CZARNY

Observatoire de Paris–Meudon, Departement d'Astrophysique Fondamentale, 5, Place Janssen, 92190 Meudon, France

The O_2^+ $b^4\Sigma_g^-$–$a^4\Pi_u$ First Negative band system has been extended to the $v = 3$ level of the upper state by photographing the (3, 1) band in high resolution. This and other newly recorded bands and the previously measured bands of this system have been reduced to molecular constants using a method to merge the least-squares results of separate band-by-band fits. First, the line positions of each are fitted separately, and second, these band-by-band results have been combined to obtain the best single values of each molecular constant of each vibrational level $v' \leq 3$ and $v'' \leq 6$. It is found that anomalies in the fine-structure splittings of the $a^4\Pi_u$ state can be accounted for fully by including the diagonal and off-diagonal elements of the phenomenological spin–spin Hamiltonian. The information contained in blended lines is partially recovered by using calculated line intensities to resolve ambiguities in their assignments. Particular attention has been paid to the strong correlation between the centrifugal distortion spin–orbit constant A_D and the spin–rotation constant γ of the $a^4\Pi_u$ state. Dunham Y_{ij} coefficients are obtained for both states. A previously unnoticed possible perturbation in the $v = 3$ level of the $a^4\Pi_u$ state has been found.

INTRODUCTION

Most of the familiar band systems of diatomic molecules involve electronic states of low to moderate multiplicities, such as singlets, doublets, or triplets. However, the O_2^+ molecule presents an outstanding exception, namely, the First Negative[1] band system, which is a transition between the $b^4\Sigma_g^-$ state and the $a^4\Pi_u$ state of this ion. Because of the common occurrence of this band system in ionization processes in oxygen (*2*) and because of the chemical reactivity of the metastable O_2^+ ($a^4\Pi_u$) ions (*3*), there is a widespread laboratory and aeronomic need for accurate values for the molecular constants of the $b^4\Sigma_g^-$ and $a^4\Pi_u$ states, so that line positions, line intensities, and populations can

[1] The designations "First Negative" and "Second Negative" for the $b^4\Sigma_g^-$–$a^4\Pi_u$ and $A^2\Pi_u$–$X^2\Pi_g$ band systems of O_2^+, respectively, have been interchanged occasionally in the published works of some of the early investigations. Tanaka and Takamine (*1*) have identified the usage in the investigations prior to 1942, the time at which the present usage appears to have established.

ISSN 0022-2852

be successfully modeled. In addition, the analysis of the O_2^+ First Negative band system is of theoretical interest because it tests how well one can predict the energy levels of electronic states of such high multiplicity. Indeed, previous analyses of this system have been unable to fit the data within the estimated experimental uncertainties.

We present here an analysis of all of the O_2^+ First Negative bands for which the rotational structure has been resolved, namely, the data of Nevin (*4*, *5*), Nevin and Murphy (*6*), Weniger (*7*), and the new bands recorded in the present investigation at the Paris–Meudon Observatory. All of these bands have been reduced to molecular constants by first fitting each band separately. These results then have been combined consistently to yield a single set of minimum-variance molecular constants for the vibrational levels $v' \leq 3$ and $v'' \leq 6$.

It is found that the previous "anomalies" in the fine-structure splittings of the $a^4\Pi_u$ state can be accounted for fully by introducing the diagonal and off-diagonal elements of the phenomenological spin–spin Hamiltonian, thus allowing one to represent the measurements within their uncertainties. In this data reduction, many of the lines that would otherwise be rejected as blends could be utilized with the aid of rotational line strengths. Particular consideration has been given to the general correlation between the centrifugal distortion spin–orbit constant A_D and the spin–rotation constant γ in the $a^4\Pi_u$ state. Attention is also drawn to a previously unnoticed possible perturbation in the $a^4\Pi_u$ state.

REVIEW OF PREVIOUS AND PRESENT DATA

The assignment of the rotational quantum numbers to the lines of the O_2^+ $b^4\Sigma_g^-$–$a^4\Pi_u$ bands, with their 48 branches, some of which are overlapped, is an extraordinarily difficult task. Fortunately, several of the important bands of this complex spectrum already have been accurately photographed and assigned. These are among those shown in Fig. 1. In 1938, Nevin (*4*) published the first high-resolution data for this band system. The measurements included the (1, 0), (0, 0), and (0, 1) bands, and in the

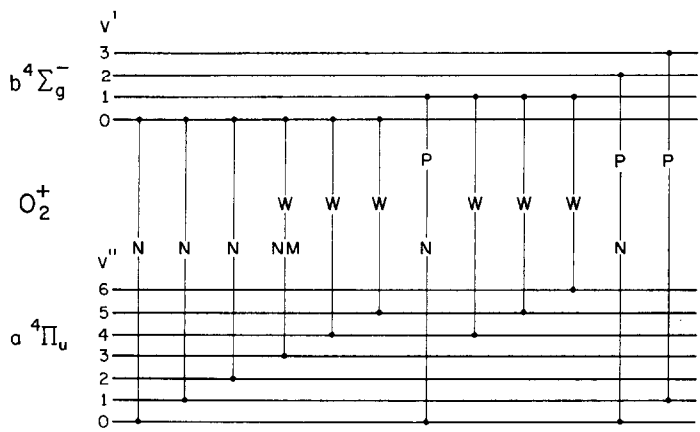

FIG. 1. Bands of the O_2^+ $b^4\Sigma_g^-$–$a^4\Pi_u$ system that have had rotational analyses. Key to symbols: N, Nevin (*4*, *5*); NM, Nevin and Murphy (*6*); W, Weniger (*7*); and P, present investigation.

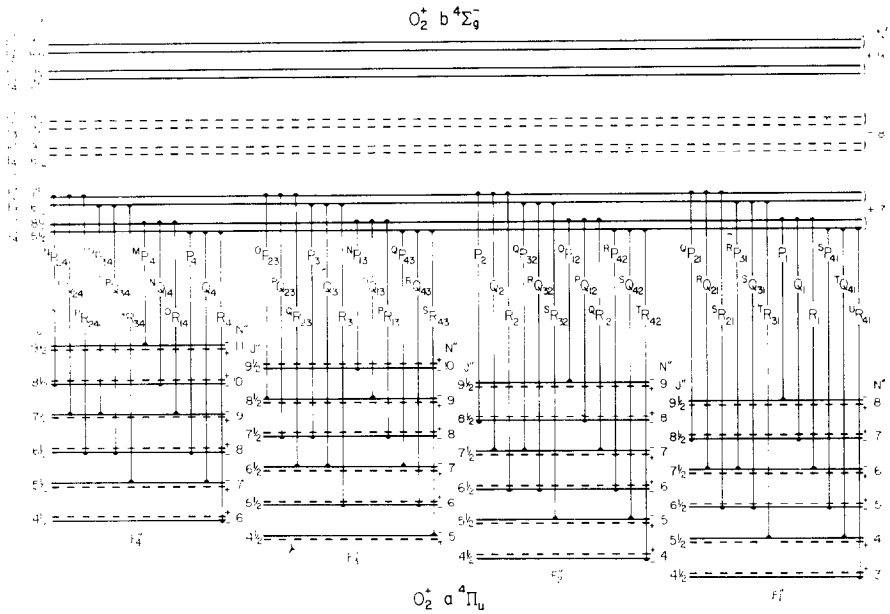

FIG. 2. Structure of the rotational energy levels of the $^{16}O_2^+$ $b^4\Sigma_g^-$ and $a^4\Pi_u$ $v = 0$ states and types of transitions that occur between these levels. The dashed lines correspond to missing levels.

following year (*5*), he added the (2, 0) and (0, 2) bands. The line positions of these latter two bands were deposited for reference in the archives of the Royal Society of London. Later, in 1941, Nevin and Murphy (*6*) reported data for the (0, 3) band. All of these spectra were excited by a discharge through helium containing a trace of oxygen and they were recorded using the second and third orders of a 21 ft grating spectrograph having resolving powers of 180 000 and 200 000, respectively. Nevin considered that the wavenumber accuracy of the measurements was about 0.04 cm^{-1}.

This band system was extended to higher vibrational levels of the $a^4\Pi_u$ state by Weniger (*7*), who in 1961 photographed the (0, 3), (0, 4), (1, 4), (0, 5), (1, 5), and (1, 6) bands, which lie to the red of the bands recorded by Nevin. The spectra were excited by a hollow-cathode discharge, cooled by liquid nitrogen, which limited the rotational development, and they were photographed with a three-prism spectrograph of reciprocal dispersion of 3 Å/mm. Weniger estimated that the wavenumbers were accurate to about 0.07 cm^{-1} (which we find, as noted below, to be too optimistic). The line positions were published for the (0, 3) and (1, 4) bands; those of the other four bands were kindly supplied to us by Weniger. Thus, the data of Nevin, Nevin and Murphy, and Weniger yield information about the vibrational levels of the $a^4\Pi_u$ state from $v'' = 0$ to $v'' = 6$. However, the knowledge of the $b^4\Sigma_g^-$ state is not as extensive; the bands of the above investigators yield information only about the first three vibrational levels $v' = 0$, 1, and 2.

Data for an additional vibrational level of the $b^4\Sigma_g^-$ state have been obtained by photographing the (3, 1) band using the Meudon Observatory solar spectrograph, which is a 7.4 m focal length f/42 Czerny–Turner mounting with a Bausch and Lomb MIT replica grating, 25.4 × 12.7 cm, ruled with 300 lines/mm. The spectra were taken

in the 11th order, which in this spectral region yields a reciprocal dispersion of about 0.21 Å/mm. The effective resolving power is about 250 000. The spectra were excited using a 2450 MHz electrodeless discharge (*8*) run in oxygen (99.995% pure) with a 6 liters/sec flow rate at a pressure of 0.05 Torr. Under these conditions and using Kodak 103ag and 103aj plates, exposures of 1 to 1.5 hr sufficed. The accuracy of the wavenumbers is estimated to be 0.03 cm^{-1}. In addition to the (3, 1) band, the (1, 0) and (2, 0) bands were also measured to serve as direct comparisons to the data of Nevin, which have similar accuracy.

STRUCTURE OF AN O_2^+ $b^4\Sigma_g^-$–$a^4\Pi_u$ BAND

Figure 2 illustrates schematically how the branches of an O_2^+ $b^4\Sigma_g^-$–$a^4\Pi_u$ band depend on the energy level structure.

In the upper $b^4\Sigma_g^-$ state, each rotational level N' consists of four closely spaced spin components denoted by F_1' ($J' = N' + \frac{3}{2}$), F_2' ($J' = N' + \frac{1}{2}$), F_3' ($J' = N' - \frac{1}{2}$), and F_4' ($J' = N' - \frac{3}{2}$). Here J' is the total angular momentum quantum number and N' is the nuclear rotation quantum number, i.e., the quantum number of the total angular momentum exclusive of spin. For a given J' value, the F' components are relatively widely separated in energy and, in the order of ascending energy, are F_1', F_2', F_3', and F_4'. On the other hand, for a given N' value, the F' components are clustered in energy and the order depends on N' and on the signs and magnitudes of the spin–spin constant ϵ_v' and the spin–rotation constant γ_v'. For the O_2^+ $b^4\Sigma_g^-$ state, the F_2' and F_3' components are nearly coincident for a given value of N', as also are the F_1' and F_4' components. Since $^{16}O_2^+$ is a homonuclear molecule composed of nuclei with zero nuclear spin, the even-valued N' levels, which have negative parity, are missing, as indicated in Fig. 2 by dashed lines. This implies that alternate J' levels of each F' component are absent.

In the lower $a^4\Pi_u$ state, spin–orbit interaction splits the state into four sublevels, denoted by F_1'' ($J'' = N'' + \frac{3}{2}$), F_2'' ($J'' = N'' + \frac{1}{2}$), F_3'' ($J'' = N'' - \frac{1}{2}$) and F_4'' ($J'' = N'' - \frac{3}{2}$). For the O_2^+ $a^4\Pi_u$ state, the sign of the spin–orbit constant A'' is negative (i.e., an inverted state); thus, in the order of increasing energy, the F_1'' component is associated with $^4\Pi_{\frac{5}{2}}$, F_2'' with $^4\Pi_{\frac{3}{2}}$, F_3'' with $^4\Pi_{\frac{1}{2}}$, and F_4'' with $^4\Pi_{-\frac{1}{2}}$, where the traditional $^4\Pi_\Omega$ designations are the Hund's case (a) limits. Here $\Omega = |\Lambda| + \Sigma$, where Λ and Σ are the projections of the orbital angular momentum and the spin angular momentum, respectively, on the internuclear axis. In addition to the above splittings, each J'' level shows Λ doubling. However, because of the above-mentioned nuclear spin statistics, all of the even (plus) parity levels are missing, as indicated by the dashed lines in Fig. 2. This implies that alternate upper and lower Λ components are missing; thus, the $^{16}O_2^+$ First Negative lines are not doublets.

As Fig. 2 shows, there are 48 branches possible in an O_2^+ First Negative band. Because of the very close coincidence (often <0.05 cm^{-1}) of the F_2' and F_3' components in the $b^4\Sigma_g^-$ state for a given N' value, eight pairs of blended branches occur, two in each subband, even in high-resolution spectra like those of Nevin (*4, 5*), Nevin and Murphy (*6*), and the present study. These high-resolution blends are summarized in Table I. Thus, there are 32 possible unblended branches and 8 blended branch pairs that constitute the 40 branches normally seen under high resolution. Note that although the

F_1' and F_4' components are also nearly coincident, no branches originating from these components are blended because they cannot connect to the same F'' rotational level.

In studies employing only moderate resolution, like that of Weniger (7), the lines associated with the F_2' and F_3' levels often cannot be separated from those associated with the F_1' and F_4' levels, which typically lie about 0.4 cm^{-1} lower for the same N' value. In such cases, as summarized in Table I, there are 8 unblended and 16 blended branch pairs or branch trios that constitute the 24 branches often seen under moderate resolution.

THEORY

In the present data reduction, the observed line positions are fit to calculated line positions found by simultaneously diagonalizing upper- and lower-state Hamiltonians with adjustable molecular constants using an iterative nonlinear least-squares procedure (9). In this section, we present the phenomenological Hamiltonians that we use and describe the calculation of their matrix elements with a Hund's case (a) basis set with a well-defined parity.

For each vibrational level of the $b^4\Sigma_g^-$ state, the phenomenological Hamiltonian may be written as a sum of four terms, arranged here in descending energy:

$$H = H_0 + H_R + H_{SS} + H_{SR}. \tag{1}$$

The first term

$$H_0 = T_V \tag{2}$$

is the electronic term value (i.e., the unsplit, nonrotating reference energy). The second term

$$H_R = B_v \mathbf{R}^2 - D_v \mathbf{R}^4 \tag{3}$$

is the rotational energy. Here $\mathbf{R} = \mathbf{J} - \mathbf{L} - \mathbf{S}$ and B_v and D_v are the rotational constant and its first centrifugal distortion correction. As shown in the next section, higher-order centrifugal distortions were not found to be necessary for the present data. The third term

$$H_{SS} = \epsilon_v(3S_z^2 - \mathbf{S}^2) \tag{4}$$

TABLE I. THE UNBLENDED, HIGH-RESOLUTION BLENDED ( ), AND MODERATE-RESOLUTION BLENDED [ ] BRANCHES OF THE O_2^+ $b^4\Sigma_g^- - a^4\Pi_u$ BAND SYSTEM

$^4\Sigma - {}^4\Pi_{-\frac{1}{2}}$	$^4\Sigma - {}^4\Pi_{\frac{1}{2}}$	$^4\Sigma - {}^4\Pi_{\frac{3}{2}}$	$^4\Sigma - {}^4\Pi_{\frac{5}{2}}$
$^NP_{14}$	$^NP_{13}$	$^OP_{12}$	P_1
$[\,^NP_{24}\ \ ^NQ_{14}]$	$[\,^OP_{23}\ \ ^OQ_{13}]$	$[\,P_2\ \ ^PQ_{12}]$	$[\,^QP_{21}\ \ Q_1\,]$
$[(\,^OQ_{24}\ \ ^OP_{34})\,^OR_{14}]$	$[(\,^PQ_{23}\ \ P_3\,)\,^PR_{13}]$	$[(\,Q_2\ \ ^QP_{32})\,^QR_{12}]$	$[(\,^RQ_{21}\ \ ^RP_{31})\,R_1\,]$
$[(\,^PR_{24}\ \ ^PQ_{34})\,P_4\,]$	$[(\,^QR_{23}\ \ Q_3\,)\,^QP_{43}]$	$[(\,R_2\ \ ^RQ_{32})\,^RP_{42}]$	$[(\,^SR_{21}\ \ ^SQ_{31})\,^SP_{41}]$
$[\,^QR_{34}\ \ Q_4\,]$	$[\,R_3\ \ ^RQ_{43}]$	$[\,^SR_{32}\ \ ^SQ_{42}]$	$[\,^TR_{31}\ \ ^TQ_{41}]$
R_4	$^SR_{43}$	$^TR_{42}$	$^UR_{41}$

TABLE II

MATRIX ELEMENTS OF THE $^4\Sigma$ HAMILTONIAN IN A PARITY CASE (a) BASIS SET[a]

$$\langle \tfrac{1}{2}\pm | H | \tfrac{1}{2}\pm \rangle = T_v + B_v(z^2 \pm 2z + 3) - D_v(z^4 \pm 4z^3 + 13z^2 \pm 12z + 6) - 3\epsilon_v - \gamma_v(\pm z + \tfrac{7}{2})$$

$$\langle \tfrac{1}{2}\pm | H | \tfrac{3}{2}\pm \rangle = (3z^2-3)^{\frac{1}{2}}\left[B_v - 2D_v(z^2 \pm z + 1) - \tfrac{1}{2}\gamma_v\right]$$

$$\langle \tfrac{3}{2}\pm | H | \tfrac{3}{2}\pm \rangle = T_v + B_v(z^2 - 1) - D_v(z^4 + z^2 - 2) + 3\epsilon_v - \tfrac{3}{2}\gamma_v$$

[a] We use the abbreviation $z = J + \frac{1}{2}$.

is the diagonal spin–spin interaction, where the spin–spin constant ϵ_v is sometimes written as λ_v, where $\epsilon_v = 2\lambda_v/3$ (*9*). Finally, the fourth term,

$$H_{\mathrm{SR}} = \gamma_v(\mathbf{J} - \mathbf{S})\cdot\mathbf{S} \tag{5}$$

is the spin–rotation interaction.

For a $^4\Sigma$ electronic state, the case (a) basis functions $|\Lambda, \Sigma\rangle$ are $|0, -\frac{3}{2}\rangle$, $|0, -\frac{1}{2}\rangle$, $|0, \frac{1}{2}\rangle$, and $|0, \frac{3}{2}\rangle$. Thus, the Hamiltonian is a symmetric 4×4 matrix and only 10 elements need be specified. However, it is more convenient to transform to a parity basis set $|\Omega\pm\rangle$, where

$$|\tfrac{1}{2}\pm\rangle = 2^{-\frac{1}{2}}[|0, \tfrac{1}{2}\rangle \pm |0, -\tfrac{1}{2}\rangle],$$
$$|\tfrac{3}{2}\pm\rangle = 2^{-\frac{1}{2}}[|0, \tfrac{3}{2}\rangle \pm |0, -\tfrac{1}{2}\rangle]. \tag{6}$$

Only states of the same parity have nonvanishing matrix elements and each 2×2 parity matrix is symmetric. Thus, the $^4\Sigma$ Hamiltonian can be specified by giving only three matrix elements. Using the notation and phase convention described in Ref. (*9*), these matrix elements are given in Table II.

For each vibrational level of the $a^4\Pi_u$ state, the phenomenological Hamiltonian may be written as a sum of five terms, written here approximately in descending energy:

$$H = H_{\mathrm{SO}} + H_{\mathrm{R}} + H_{\mathrm{SS}} + H_{\mathrm{SR}} + H_{\Lambda}. \tag{7}$$

The first term

$$H_{\mathrm{SO}} = A_v L_z S_z + \tfrac{1}{2}A_{Dv}(\mathbf{R}^2 L_z S_z + L_z S_z \mathbf{R}^2) \tag{8}$$

is the spin–orbit interaction and a centrifugal distortion correction that arises as a cross term between $A(r)L_zS_z$ and H_{R}. The constant A_{Dv} is sometimes written as A_J, where

TABLE III. MATRIX ELEMENTS OF THE $^4\Pi$ HAMILTONIAN IN A PARITY CASE (a) BASIS SET[a]

$$\langle \tfrac{5}{2}\pm|H|\tfrac{5}{2}\pm\rangle = T_v + \tfrac{3}{2}A_v + 3\epsilon_v + \tfrac{1}{2}q_v + (B_v + \tfrac{3}{2}A_{Dv} + \tfrac{1}{2}q_v)(z^2-5) - D_v(z^4 - 7z^2 + 13)$$

$$\langle \tfrac{5}{2}\pm|H|\tfrac{3}{2}\pm\rangle = (3)^{\frac{1}{2}}(z^2-4)^{\frac{1}{2}}\left[B_v + A_{Dv} - \tfrac{1}{2}\gamma_v + \tfrac{1}{2}q_v + \tfrac{1}{4}p_v - 2D_v(z^2-2)\right]$$

$$\langle \tfrac{5}{2}\pm|H|\tfrac{1}{2}\pm\rangle = -(12)^{1/2}D_v(z^2-1)^{1/2}(z^2-4)^{1/2}$$

$$\langle \tfrac{5}{2}\pm|H|-\tfrac{1}{2}\pm\rangle = \pm\tfrac{1}{2}q_v(z^2-1)^{1/2}(z^2-4)^{1/2}$$

$$\langle \tfrac{3}{2}\pm|H|\tfrac{3}{2}\pm\rangle = T_v + \tfrac{1}{2}A_v - 3\epsilon_v - 3\gamma_v + \tfrac{1}{2}q_v + \tfrac{3}{2}p_v + 3o_v + (B_v + \tfrac{1}{2}A_{Dv} + \tfrac{1}{2}q_v)(z^2+1) - D_v(z^4 + 9z^2 - 15)$$

$$\langle \tfrac{3}{2}\pm|H|\tfrac{1}{2}\pm\rangle = 2(z^2-1)^{1/2}\left[B_v - \tfrac{1}{2}\gamma_v + \tfrac{1}{2}q_v + \tfrac{1}{4}p_v \pm \tfrac{1}{4}q_v z - 2D_v(z^2+2)\right]$$

$$\langle \tfrac{3}{2}\pm|H|-\tfrac{1}{2}\pm\rangle = (3)^{1/2}(z-1)^{1/2}\left[\pm(q_v + \tfrac{1}{2}p_v) - 2D_v z\right]$$

$$\langle \tfrac{1}{2}\pm|H|\tfrac{1}{2}\pm\rangle = T_v - \tfrac{1}{2}A_v - 3\epsilon_v - 4\gamma_v + \tfrac{1}{2}q_v + 2p_v + 4o_v + (B_v - \tfrac{1}{2}A_{Dv} + \tfrac{1}{2}q_v)(z^2+3) \pm (2q_v + p_v)z - D_v(z^4 + 13z^2 + 5)$$

$$\langle \tfrac{1}{2}\pm|H|-\tfrac{1}{2}\pm\rangle = (3)^{1/2}\left[\pm(\alpha_v + q_v + p_v + 2o_v) + (B_v - \tfrac{1}{2}\gamma_v - A_{Dv} + \tfrac{1}{2}q_v + \tfrac{1}{4}p_v)z - 2D_v z(z^2+2)\right]$$

$$\langle \tfrac{1}{2}\pm|H|-\tfrac{1}{2}\pm\rangle = T_v - \tfrac{3}{2}A_v + 3\epsilon_v - 3\gamma_v + \tfrac{1}{2}q_v + \tfrac{3}{2}p_v + 3o_v + (B_v - \tfrac{3}{2}A_{Dv} + \tfrac{1}{2}q_v)(z^2+1) - D_v(z^4 + 5z^2 + 1)$$

[a] We use the abbreviation $z = J + \frac{1}{2}$.

$A_{Dv} = 2A_J$ (*10, 11*). The second term H_R is defined as in Eq. (3). The third term,

$$H_{SS} = \epsilon_v(3S_z^2 - \mathbf{S}^2) + \tfrac{1}{2}\alpha_v(S_+S_+ + S_-S_-)\delta_{0,\Delta\Omega}, \tag{9}$$

is both the diagonal spin-spin interaction (see Eq. (4)) and the off-diagonal spin-spin interaction, which is most familiarly recognized as the source of the J-independent Λ doubling of the $\Omega = 0$ component of a $^3\Pi$ state. The fourth term H_{SR} is defined as in Eq. (5). Finally, the fifth term

$$H_\Lambda = \tfrac{1}{2}q_v(J_+ + J_-)^2 - (\tfrac{1}{2}q_v + \tfrac{1}{4}p_v)[(J_+ + J_-)(S_+ + S_-) + (S_+ + S_-)(J_+ + J_-)] + (\tfrac{1}{2}q_v + \tfrac{1}{2}p_v + o_v)(S_+ + S_-)^2 \tag{10}$$

is the effective Λ-doubling interaction expressed in terms of the three well-known constants q_v, p_v, and o_v. As explained in Ref. (*9*), o_v cannot be extracted from experimental data and we use the approximation

$$o_v = \tfrac{1}{8}(A_v/B_v)p_v. \tag{11}$$

The use of effective operators for the Λ-doubling interaction appears not to have been given before. The derivation of Eq. (10) is a straightforward application of the Van Vleck transformation (*9*).

For the $a^4\Pi_u$ state, there are eight case (a) basis functions of the form $|\Lambda, \Sigma\rangle$, and they may be transformed to a parity basis set $|\Omega\pm\rangle$ of the form

$$\begin{aligned} |\tfrac{5}{2}\pm\rangle &= 2^{-\frac{1}{2}}[|1, \tfrac{3}{2}\rangle \pm |-1, \tfrac{3}{2}\rangle], \\ |\tfrac{3}{2}\pm\rangle &= 2^{-\frac{1}{2}}[|1, \tfrac{1}{2}\rangle \pm |-1, -\tfrac{1}{2}\rangle], \\ |\tfrac{1}{2}\pm\rangle &= 2^{-\frac{1}{2}}[|1, -\tfrac{1}{2}\rangle \pm |-1, \tfrac{1}{2}\rangle], \\ |-\tfrac{1}{2}\pm\rangle &= 2^{-\frac{1}{2}}[|1, -\tfrac{3}{2}\rangle \pm |-1, \tfrac{3}{2}\rangle]. \end{aligned} \tag{12}$$

With this basis set, the $^4\Pi$ Hamiltonian is a 4×4 symmetric matrix and can be specified by 10 matrix elements, which are derived[2] using Ref. (*9*) and are listed in Table III.

[2] There is a typographical error in the second matrix element of Table II of Ref. (*9*). The sign in front of A_{Dv} should be a plus instead of a minus.

Previously, both Nevin (*4–6*) and Weniger (*7*) used in the reduction of their data the theoretical energy level expressions derived by Budó (*12*) for a $^4\Sigma$ state and by Brandt (*13*) for a $^4\Pi$ state. While the energy levels of the $^4\Sigma$ state appeared to be well represented by Budó's formulas, Nevin noted that the representation was unsatisfactory for the $^4\Pi$ state. Budó and Kovács (*14*) made the first attempt to remove this discrepancy by considering the perturbations of the $^4\Pi_u$ fine structure resulting from *two* $^2\Pi_u$ states and found that the discrepancies could be thereby reduced. Later, Kovács (*15*) found that the diagonal part of the spin–spin interaction, $\epsilon_v(3S_z^2 - \mathbf{S}^2)$, produces the same effect on the separation of the multiplets as do the perturbations caused by the two $^2\Pi_u$ states; thus, the two effects cannot be distinguished. This treatment was also applied to Weniger's data (*7*) by Kovács and Weniger (*16*), where they showed that the residuals between observed and calculated energy levels for the $a^4\Pi_u$ state could be reduced thereby to about 0.3 cm^{-1} for the data of Nevin (*4–6*) and about 1 cm^{-1} for the data of Weniger (*7*), judging from the figures in their paper. Thus, the introduction of the phenomenological diagonal spin–spin parameter ϵ_v reduces the discrepancies, but the remaining residuals are nevertheless still an order of magnitude larger than the accuracy of the experimental data.

None of these studies considered the off-diagonal spin–spin interaction characterized by the constant α_v in Table III. We find it essential to include this interaction in the $^4\Pi$ Hamiltonian in order to fit the data within their experimental uncertainties. Veseth (*17*) independently reached the same conclusion about the same time. With a similar term in the $^4\Pi_u$ Hamiltonian, he fit $a^4\Pi_u$ term values based on Nevin's data (*4–6*) alone to a 0.054 cm^{-1} rms deviation, typically. Furthermore none of the earlier studies simultaneously included the constants A_{Dv} and γ_v in the $^4\Pi$ Hamiltonian. Although these constants are less important to the quality of the representation than α_v, we have given them special attention.

The resulting $^4\Sigma$ and $^4\Pi$ Hamiltonians used here represent the high-resolution data of Nevin (*4–6*) and those of the present study to a 0.031 cm^{-1} standard deviation, which is at least about a factor of two smaller than previous studies.

DATA REDUCTION

Since the bands of Nevin (*4, 5*), Nevin and Murphy (*6*), and Weniger (*7*) already had rotational assignments, these bands were the first to be reduced to molecular constants for $v' \leq 2$ and $v'' \leq 6$ using the techniques described below. The lines of the (1, 0) and (2, 0) bands recorded in the present study were assigned by comparing the observed wavenumbers to the positions and relative intensities predicted by the above molecular constants. The agreement with the measured wavenumbers of Nevin (*4, 5*) for commonly measured lines is excellent. For the newly recorded (3, 1) band, the assignments were made in the following way. The above molecular constants for the upper state were extrapolated with fitted $v' + \frac{1}{2}$ polynomonials to obtain values associated with $v' = 3$, which together with the above values for $v'' = 1$, were used to predict the locations and relative intensities of the lines of the (3, 1) band. By comparing these predicted positions and intensities to the positions of the measured lines, the structure of the main branches of the band could be easily identified. The assignments were checked with combination differences. These major lines of the band were then reduced to molecular constants,

which then could be used straightforwardly to identify the weaker lines of this band in an incremental iterative fashion. The resulting assignments and measured wavenumbers of the (3, 1) band are given in Table IV.[3]

The reduction of the lines of all of the O_2^+ First Negative bands to molecular constants has several special features. Many of the branches are blended in systematic and varying degrees. Some reassignment of the lines measured in previous investigations was required and a few lines had to be rejected as unexplained "outliers." Finally, a statistically significant set of molecular constants had to be selected from the numerous constants possible for $^4\Sigma$ and $^4\Pi$ states. These details are summarized here. (Some lines also had to be omitted from the fit due to a possible perturbation, which is discussed in a later section.)

Treatment of Blends

One of the most vexing problems in the assignment of lines is the presence of "blends," whereby two or more lines are so close in wavenumber position compared to the resolution that the assignment appears at first glance to be ambiguous. We describe here the use of calculated line intensities in order to recover, in part, the information contained in blended lines.

The blends encountered in the O_2^+ First Negative bands predominantly arise from the very small separation of the F_2' and F_3' components, as indicated in Fig. 2 and Table I. Since both this separation and the intensity of the blended lines vary considerably for the low J'' lines, the proper assignment of the lines associated with these components is nontrivial. This is illustrated in Figs. 3 and 4 for the $^QQ_{24}$–$^QP_{34}$ and the $^QR_{23}$–Q_3 blends, respectively. The intensities of the two blended lines are indicated by vertical bars. The separations of the two lines, which are of course the separation of the F_2' and F_3' components, are given numerically above the bars and the larger separations are shown schematically by gaps between the bars. The intensities are based on the eigenvectors obtained by direct computer diagonalization (*18*) of the molecular Hamiltonians with the constants listed below for the (3, 1) band and using population factors appropriate to 500 K. The separations are, of course, the differences between the accompanying eigenvalues.

The separation is relatively wide, 0.767 cm^{-1}, at $N' = 1$ but rapidly narrows to less than 0.05 cm^{-1} for most of the lines encountered in Table IV. The F_2' and F_3' components are essentially coincident at $N' = 27$, above which the energy location of the two components is reversed. Accompanying this, the relative intensities of the lines are also changing rapidly for the lines associated with the lower J'' values. Figure 3 shows that the $^QQ_{24}$ lines vastly predominate for the first few lines, but are less intense than the $^QP_{34}$ lines at high J'' levels. Similarly, Fig. 4 shows that the relative intensity of the $^QR_{23}$ and the Q_3 lines also reverses along the branches.

The interplay of the varying intensity and varying separation determines which resolved or blended lines are likely to be observed. Figure 3 shows that, although the first pair of lines are widely separated and easily resolved, the relative intensities are so disproportionate that only the $^QQ_{24}(1\frac{1}{2})$ line would be expected to be present. Although

[3] The line positions of the (1, 0) and (2, 0) bands measured in the present study are on deposit in the Editorial Office of the Journal of Molecular Spectroscopy and can be made available on request.

TABLE IV A. WAVENUMBERS OF THE MEASURED LINES IN THE O_2^+ (3,1) FIRST NEGATIVE BAND. $^4\Sigma - {}^4\Pi_{-1/2}$ SUB-BAND.

J+1/2	N P 24	O Q 24	P R 24	O P 34	P Q 34	Q R 34	M P 14	N Q 14	O R 14	P 4	Q 4	R 4
1			0		0							0
2		18961.084		0		18972.965			18960.684		0	
3	0		18967.420		18967.256			0		0		18985.6028
4		18959.289		0		18980.919	18946.713		18958.840		18980.499	
5	18949.050		18970.827		18970.691			18948.611		18970.252		19001.670
6		18957.982		18957.893		18989.387B		0			18988.943B	
7	18943.206		18974.633		18974.562			18942.695		18974.099B		19015.190
8		18957.207B		0		18998.209					0	
9	18937.991		0		18978.947			18937.461B		18978.501		19029.237
10		18956.959B		0		19007.626					19007.197	
11	18933.159		0		18983.872B			0		18983.396		19043.865
12		0		18957.313B		19017.630					19017.213	
13	18929.094		0		18989.387B			0		18988.943B		19058.993
14		0		18958.320B		19028.294					19027.872	
15	18925.621		0		18995.564			0		18995.132		19074.755
16		0		18959.993B		19039.594					19039.188	
17	18922.875		0		19002.458			0		19002.011		19091.120
18		0		18962.439B		19051.567					19051.154	
19	18920.828		0		19009.956			0		19009.530B		19108.324
20		0		18965.497		19064.248					19063.836	
21	18919.498		0		19018.274			0		19017.872		19126.118B
22		0		18969.412		19077.682					19077.279	
23	0		0		19027.395			0		19026.989		19144.772
24		0		18974.099B		19091.863B					19091.496	
25	0		0		19037.433R			0		19037.004R		19164.129B
26		0		18979.624		19106.677B					19106.508	
27	0		0		19048.007			0		19047.616		19184.314
28		0		18986.009		19122.747					19122.331	
29	0		0		0			0		19059.186B		19205.234
30		0		0		0					0	
31	0		0		0			0		19071.503		0
32		0		0		0					0	
33	0		0		0			0		0		0
34		0		0		0					0	

0 = ALLOWED LINE, BUT NOT OBSERVED.

B = BLENDED LINE, NOT INCLUDED IN THE FIT.

R = STATISTICALLY REJECTED LINE, NOT INCLUDED IN THE FIT.

TABLE IV B. WAVENUMBERS OF THE MEASURED LINES IN THE O_2^+ (3,1) FIRST NEGATIVE BAND. $^4\Sigma - {}^4\Pi_{1/2}$ SUB-BAND.

J+1/2	O P 23	P Q 23	Q R 23	P 3	Q 3	R 3	N P 13	O Q 13	P R 13	Q P 43	R Q 43	S R 43
1			0		0							19025.421B
2		0		0		19022.619			19010.222		19022.120	
3	0		0		19017.103			19004.746		19016.540		19038.440B
4		19009.5303		0		19031.145	0		19009.041B		19030.715	
5	18999.581		19021.251		19021.167			18999.052		19020.7738		19052.178
6		19009.3118		0		0	18987.045		19008.725B		19040.159	
7	18994.746		19026.183		0			18994.305		19025.692		19066.789
8		19009.733		0		0	18977.915		19009.311B		19050.412	
9	18990.866		19031.978		0			18990.447		19031.508		19082.252
10		19011.1673		0		0	18969.674		19010.751		19061.485	
11	18987.366		19038.569		0			18987.460		19038.200		19098.592B
12		19013.529		0		0	18962.339		19013.099		19073.434	
13	18985.897		19046.199		0			18985.382		19045.752		19115.732
14		19016.659		0		0	18955.959		19016.232		19086.260	
15	18984.6183		19054.652B		0			18984.207		19054.201		19133.789
16		19020.7738		0		19100.370	18950.389		19020.346		19099.961	
17	18984.353		19063.947B		0			18983.872B		19063.508		19152.707
18		19025.634		0		19115.008	18945.795		19025.421B		19114.554	
19	18985.046		19074.179		0			18984.618B		19073.760		19172.513
20		19031.710		0		19130.314B	18942.076		0		19129.902B	
21	18986.611		0		19085.321B			18986.117		19084.912		19193.154
22		19038.4403		0		19146.831	18939.480		19038.040		19146.417	
23	18989.114		0		19097.378			18988.602B		19096.960		19214.736
24		19046.347		0		19164.129B	18937.461B		0		0	
25	18992.585		0		19110.357			0		19109.939		19237.196
26		19055.069		0		19182.298	0		0		19181.899	
27	18996.995		0		19124.257			0		19123.824		19260.545
28		19064.672		0		19201.330	0		0		19200.970	
29	19002.394		0		19139.117			0		19138.710		0
30		19075.250		0		0	0		0		0	
31	19008.729B		0		19154.638R			0		0		0
32		0		0		0	0		0		0	
33	19015.553R		0		0			0		0		0
34		0		0		0	0		0		0	

0 = ALLOWED LINE, BUT NOT OBSERVED.

B = BLENDED LINE, NOT INCLUDED IN THE FIT.

R = STATISTICALLY REJECTED LINE, NOT INCLUDED IN THE FIT.

TABLE IV C. WAVENUMBERS OF THE MEASURED LINES IN THE O_2^+ (3,1) FIRST NEGATIVE BAND. $^4\Sigma - {}^4\Pi_{3/2}$ SUB-BAND.

J+1/2	P 2	Q 2	R 2	Q P 32	R Q 32	S R 32	O P 12	P Q 12	Q R 12	R P 42	S Q 42	T R 42
1												
2		0		19059.924B		0			0		19072.265B	
3	0		0		19067.720R			0		19067.136		0
4		0		19059.924B		0	19047.815		19059.643B		19081.476	
5	0		0		19072.457			0		0		0
6		0		19060.830		19092.266	19038.440B		19060.514		19091.863B	
7	0		0		19078.515			0		19078.085		19119.233
8		0		19062.647		19103.659	19030.849		19062.285		19103.243B	
9	19044.692		0		19085.753			19044.278		19085.321B		19136.372
10		0		19065.659		19116.360	19024.182		19065.236		19115.943	
11	0		0		19094.125			0		19093.711		19154.100
12		0		19069.764		19130.130	19018.601		19069.361		19129.724	
13	19043.279		0		19103.739R			19042.911		19103.243B		0
14		0		19074.957B		19145.046	19014.227		19074.650		19144.629	
15	0		0		19114.420B			0		0		19193.471
16		0		19081.555B		19161.036B	19011.167B		19081.043		19160.626	
17	19046.542		0		19126.118B			19046.102		19125.687B		19214.831
18		0		19088.995B		19178.158	19009.041B		19088.562		19177.717	
19	19049.821		0		19138.967			19049.353		19138.543		19237.285
20		0		19097.614		19196.330	19007.976		19097.176		19195.925	
21	0		0		19152.900			19053.732		0		0
22		19107.317		0		19215.557	19008.109		19106.877B		19215.157	
23	19059.643B		0		19167.904			19059.186B		0		0
24		19118.0763		0		19235.908	19009.3118		19117.631		0	
25	19066.141		0		19183.959			19065.703		0		0
26		19130.024R		0		19257.181	19011.640		19129.543		0	
27	0		0		19200.971			19073.316		0		0
28		19142.737		0		19279.463	19015.168		0		0	
29	19082.370		0		19219.049			19081.942		0		0
30		19156.7278		0		0	0		19156.294B		0	
31	19092.051		0		0			19091.609		0		0
32		0		0		0	0		0		0	
33	0		0		0			0		0		0
34		0		0		0	0		0		0	

0 = ALLOWED LINE, BUT NOT OBSERVED.

B = BLENDED LINE, NOT INCLUDED IN THE FIT.

R = STATISTICALLY REJECTED LINE, NOT INCLUDED IN THE FIT.

TABLE IV D. WAVENUMBERS OF THE MEASURED LINES IN THE O_2^+ (3,1) FIRST NEGATIVE BAND. $^4\Sigma - {}^4\Pi_{5/2}$ SUB-BAND.

J+1/2	Q P 21	R Q 21	S R 21	R P 31	S Q 31	T R 31	P 1	Q 1	R 1	S P 41	T Q 41	U R 41
1												
2												
3	19106.163		0		19118.0768			19105.723		0		0
4		19111.111		19110.920		0	19098.592B		0		0	
5	19101.999		0		19123.640			19101.528		0		19154.648
6		19112.584		0		19143.897	19090.427		19112.188		0	
7	19099.247R		19130.859		19130.773			19096.790B		19130.314B		0
8		19115.622		0		19156.727B	19083.774		19115.222		19156.2943	
9	0		19139.433B		0			19097.934		0		0
10		19120.143B		0		19170.848	19078.632		19119.717		0	
11	19098.790B		19149.518B		0			19098.366		0		0
12		19126.118B		0		19186.467	19074.957B		19125.687B		0	
13	19100.604		19161.036B		0			19100.222		0		0
14		19133.506		0		19203.433	19072.700		19133.068		0	
15	19103.917		19173.905B		0			19103.476		0		0
16		19142.246		0		19221.784	19071.813		19141.804		0	
17	19108.522		19188.119B		0			19108.073		0		0
18		19152.299		0		19241.424	19072.265B		19151.860		0	
19	19114.420B		19203.570		0			19113.978		0		0
20		19163.647		0		0	19074.012		19163.183		0	
21	19121.600		19220.294		0			19121.147		0		0
22		19176.200		0		0	19077.003		19175.748		0	
23	19129.902B		19238.015B		0			19129.449		0		0
24		19189.970		0		0	19081.235		19189.509		0	
25	19139.433B		19257.307		0		0			0		0
26		19204.641		0		0	19086.638		19204.394		0	
27	19150.341		19277.555		0			19149.877		0		0
28		19220.899		0		0	19093.217		19220.438		0	
29	19162.202		19298.863		0			19161.773		0		0
30		19238.0193		0		0	19100.943		19237.573		0	
31	19175.233		0		0			19174.777		0		0
32		0		0		0	19109.766		0		0	
33	0		0		0			0		0		0
34		0		0		0	0		0		0	

0 = ALLOWED LINE, BUT NOT OBSERVED.

B = BLENDED LINE, NOT INCLUDED IN THE FIT.

R = STATISTICALLY REJECTED LINE, NOT INCLUDED IN THE FIT.

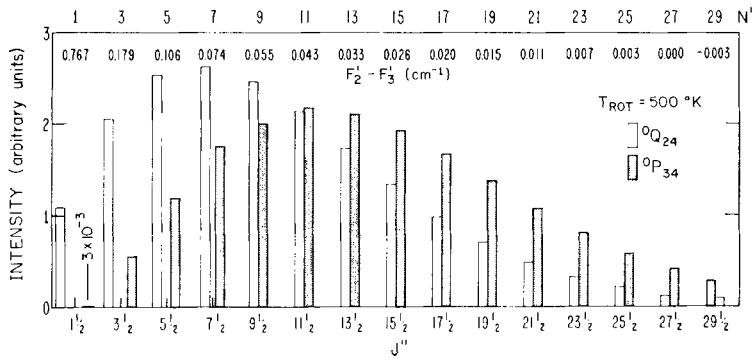

FIG. 3. Calculated relative intensities and separations of the $^{0}Q_{24}$ and $^{0}P_{34}$ lines of the (3, 1) band.

not as extreme, Fig. 4 shows a similar situation. For the next few J'' levels, both lines should often be present and resolved; see, for example, the lines $^{Q}R_{23}(4\frac{1}{2})$ and $Q_3(4\frac{1}{2})$ in Table IVB and Fig. 4. When the separation drops to less than 0.06 cm^{-1}, we have found that the lines cannot be resolved in the investigations considered here.

However, when the intensity pattern is like that in Fig. 4, many of the blended lines are practically only one line, because of either the widely different relative intensities or the nearly zero separation (or, of course, both). Specifically, it was found that, first, when the intensity ratio is greater than about 5:1, the "blend" could be measured just as accurately as an unblended line regardless of the separation. In such cases, the measured line position was assigned to the brighter line; see, for example, the line $^{Q}R_{23}(10\frac{1}{2})$ in Fig. 4 and Table IVB. Secondly, it was found that when the separation was less than about half of the standard deviation of the residuals of the fit σ ($\sigma/2 = 0.016$ cm^{-1} for the (3, 1) band),[4] the "blend" could again be measured just as accurately as an unblended line regardless of the ratio of intensities. In such cases, the measured line position was assigned to the brighter line; see, for example, the line $^{0}P_{34}(19\frac{1}{2})$ in Fig. 3 and Table IVA. One could also, in fact, consider that, when the intensities of two such lines are comparable, *both* of the lines could be used in the fit with the same wavenumber. Although this may be preferable, we adopted the simpler course of using only one line with each wavenumber.

A second class of blends encountered here was the "accidental" overlap of lines of the same band that are associated with different J''. In these cases, the calculated intensities and separation were again used as guides in assigning the measured wavenumber in the same fashion described above. For example, the relative intensities of the lines $Q_4(11\frac{1}{2})$ and $^{Q}R_{23}(2\frac{1}{2})$ in the (3, 1) band are estimated to be in the ratio 9:1 and have a separation of 0.027 cm^{-1}. As a result, the measured wavenumber is assigned to the former in Table IVA and the latter has no entry in Table IVB.

Thus in this fashion, many of the "blended" lines could be used without loss of accuracy in the determination of the molecular constants, thereby adding somewhat to

[4] It is common and often useful statistical notation to distinguish between the quantity being estimated and the value obtained as the estimate, like σ here, by placing a circumflex over the latter. The distinction does not seem useful here, and to simplify the notation, it is not made.

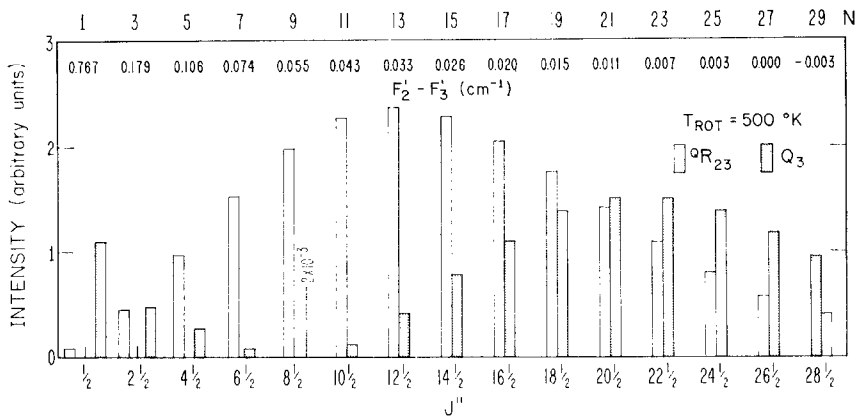

FIG. 4. Calculated relative intensities and separations of the $^QR_{23}$ and Q_3 lines of the (3, 1) band.

the precision of these values. The blends between two or more (3, 1) lines that did not meet the above criteria were not included in the fit and are identified accordingly in Table IV. Naturally, this technique requires that the estimated relative intensities and separations be realistic. The relative intensities, which do not depend sensitively on small changes in the molecular constants, have been found (*18*) to compare very adequately with the average of the intensity estimates made by Nevin (*4*, *5*) and Nevin and Murphy (*6*). A temperature of 500 K was assumed to be representative throughout. We found that the intensity ratios of blended lines were not unduly sensitive to a reasonable choice of temperature. In estimating separations, one intially had to use a preliminary set of molecular constants, but these estimates were always rechecked using a nearly final set of constants. Very few changes were required in the selection of which blends could or could not be used.

Lastly, one type of blend could not be handled straightforwardly with this technique, namely, those lines that are "accidentally" overlapped with lines of another band associated with a different v'. For example, the (3, 1) band lies in the same wavelength region as the (2, 0) band. Relative intensities are difficult to estimate realistically in such a situation because of the virtually unknown ratio of populations in the two upper vibrational levels. However, the estimated separation could be used as a warning that there may be difficulties associated with the measurement due to blending. For example, the $^OP_{23}(32\frac{1}{2})$ line of the (3, 1) band is separated from the $^RQ_{32}(10\frac{1}{2})$ line of the (2, 0) band by about 0.087 cm^{-1} and this may be the reason why the wavenumber assigned to the $^OP_{23}(32\frac{1}{2})$ line gave an unacceptably large residual in the fit. In a few such cases where it seemed fairly clear that a line position measurement was inaccurate due to a blend with the line of another band, both were omitted from the fit.

Reassigned Lines

Because of this complicated interplay of varying separation and intensities for the low N' values, the assignment of these lines in the earlier studies must have been extremely difficult. A few misassignments were indeed found. For example, the line observed at 17 756.82 cm^{-1} in the (1, 0) band was assigned to $^PQ_{34}(\frac{1}{2})$ by Nevin (*4*).

However, when this assignment was used, a residual of 0.7 cm^{-1} occurred in the fit. It is much more reasonable that this wavenumber belongs to the nearby "blend" (see Table I) $^PR_{24}(\frac{1}{2})$, since the intensity of the $^PR_{24}(\frac{1}{2})$ line is predicted to be 1000 times greater than that of the $^PQ_{34}(\frac{1}{2})$ line. Furthermore, with this reassignment, the residual drops to 0.01 cm^{-1}.

Statistically Rejected Lines

In the fitting of each of the bands there were a few lines that were poorly represented, regardless of the type of constants used in the upper- and lower-state models. These "outliers" were rejected using the relatively simple Chauvenet's criterion (*19*), which is based on the estimated standard deviation σ and the number of observed lines n. Residuals are rejected that have a (normal) probability of only $1/2n$ of occurring. In the (3, 1) band, for example, the rejection point was $\pm 3.2\sigma$, or about 0.11 cm^{-1}. There were only eight rejected lines; no reason could be found for the misfits. These lines are identified accordingly in Table IV. Removing these measurements from the set of 338 lines reduced the standard deviation from 0.0386 to 0.0316 cm^{-1}.

Selection of the Molecular Constants

As indicated in the section above, the set of possible types of molecular constants for $^4\Sigma$ and $^4\Pi$ electronic states is unusually large: $\nu_0(v', v'')$, B', D', γ', ϵ', A'', A_D'', B'', D'', γ'', ϵ'', q'', p'', α'', and higher-order centrifugal distortion constants like H', H'', γ_D', q_D'', p_D'', etc. The problem is to select from this set of all possible constants the subset that is statistically significant for the present data.

a. Use of the F-Test

This was done with the aid of the F-test (*20*), which, in this application, allows one to either accept or reject, with a chosen confidence level, the possibility that the unknown "true" values of one or more molecular constants are zero. If it is likely that the tested constants are zero, then they are omitted from the Hamiltonians. On the other hand, if the possibility that the tested constants are zero is rejected, then they are included in the Hamiltonians. The F-test compares an experimental F_e value, which is determined from the molecular constants and variance–covariance matrix (*21*, Section D-2-c) of the least-squares fit made with the constant in question included, to tabulated F values. If $F_e \leq F$, then one accepts the possibility that the "true" values of the tested constants are zero. If $F_e > F$, then one rejects this possibility. Tabulated $F(\nu_1, \nu_2, 1 - \alpha)$ depend on the number of tested constants ν_1, the degrees of freedom of the least-squares fit ν_2, and the selected chance α of accidently rejecting the possibility when indeed it is actually true. For the relatively large degrees of freedom encountered here and a $1 - \alpha = 0.95$ significance level, the tabulated F values are 3.9 for testing one constant[5] and 3.0 for testing two constants.

[5] For one constant, the F-test is exactly equivalent to the perhaps better known t-test (*21*, Section D-3), where the 100 $(1 - \alpha)\%$ confidence interval of a fitted constant is examined to see if it includes zero. The reason for the equivalence is that $t(n - m, 1 - \alpha) = [F(1, n - m, 1 - \alpha]^{\frac{1}{2}}$. The t-test, however, is not applicable to two or more constants simultaneously with nonzero covariances.

TABLE V. F-TESTS OF THE MOLECULAR CONSTANTS H', H'', γ', A_D'', γ'', q'', AND p'' FOR THE HIGH-RESOLUTION FIRST NEGATIVE O_2^+ BANDS[a]

band[b]	degrees of freedom	$H'(10^{-11})$	$H''(10^{-11})$	$F_e(H',H'')$	$\gamma'(10^{-4})$	$F_e(\gamma')$	$F_e(A_D'',\gamma'')$	$F_e(q'',p'')$
(0,0)N	276	4.0(9.4)	7.7(8.2)	4.59	-2.1(1.5)	1.86	68.8	240
(0,1)N	289	-5.1(7.8)	-3.8(7.7)	1.09	-6.9(1.7)	16.5	103	238
(0,2)N	338	6.3(6.0)	8.1(6.0)	1.80	-6.3(1.6)	15.9	100	324
(0,3)NM	285	-2.4(9.1)	1.7(8.5)	2.04	-5.6(1.5)	14.5	66.8	220
(1,0)N	303	-8.3(8.2)	-7.3(8.5)	0.622	-6.2(1.9)	10.8	56.9	133
(1,0)P	328	-6.2(7.2)	-2.5(7.1)	2.69	-5.7(1.2)	21.1	158	321
(2,0)N	209	-12(29)	-15(30)	0.165	-10.3(2.9)	12.9	36.2	58.1
(2,0)P	179	24(27)	23(29)	0.427	-5.4(2.4)	5.28	47.8	101
(3,1)P	314	13(24)	5(23)	0.321	-9.6(1.8)	27.4	70.9	103

[a] All units are reciprocal centimeters. The F_e value is dimensionless. The number in parentheses corresponds to one standard error expressed in terms of the last digits, i.e., $4.0(9.4)\times10^{-11} = (4.0\pm9.4)\times10^{-11}$.

[b] N = Nevin (4, 5), NM = Nevin and Murphy (6) and P = present study.

The testing was done for the First Negative data in the following way. All of the molecular constants that could conceivably be appropriate for these data were fitted to several bands individually. The constant that the F-test showed to be determined with the *least* confidence was dropped, the fit made again, and the testing thus repeated until a set of constants remained whose "true" values could be said to be different from zero with a high level of confidence.

Table V lists the results of the F-test applied to the more poorly determined constants of the high-resolution bands. The most poorly determined constants are the elusive rotational centrifugal distortion constants H' and H'', which require very precise and/or very rotationally extensive data to be significant. For the present data, the Dunham expression (*22*) yields $H'' \approx -5 \times 10^{-12}$ cm^{-1} and $H' \approx -2 \times 10^{-11}$ cm^{-1}. For the highest J levels, the H_v contribution to the term energies would then be 0.09 and 0.32 cm^{-1}, respectively. Thus, it would be unreasonable to assume, without testing, that these constants were not significant. Consequently, fits were made to the high-resolution bands with Hamiltonians that included the H_v matrix elements (*23*) and the resulting fitted values tested. Table V shows that the standard errors of these fitted values of these constants are all as large, or larger, than the values themselves. Thus, one immediately suspects that each of the constants *separately* is not too significant in these individual band fits. However, to ask whether *both* can be zero simultaneously requires the F-test, whose use of the covariance (*21*, Section D-2-c) accounts for the high correlation between these two constants. The calculated $F_e(H', H'')$ values in Table V are almost all less than the critical value of $F = 3.0$. The only exception is the (0, 0) band, which is *not* the band of highest J level. We conclude from this that H_v' and H_v'' are not required, or at most, only very marginally required, by the present data and omit these constants from the Hamiltonian. Further, such tests made using all of the bands taken together, as described below, support this choice.

Table V also shows the fitted values, standard errors, and F-tests for the upper-state spin–rotation constant γ'. The standard errors are all several times smaller than the fitted values, suggesting that γ' is significant for these data. The F-tests certainly support

this, since almost all of the calculated F_e values are larger than the critical value of $F = 3.9$. Thus, there appears to be little doubt about including γ' in the Hamiltonian.

Also listed in Table V are the F-tests for the lower-state spin–orbit centrifugal distortion spin–rotation constant A_D'' and the constant γ''. These constants are tested as a pair simultaneously because it is difficult to obtain meaningful fitted values of these two separately. This is due to the extremely high correlation that exists between these two parameters in the $^4\Pi$ Hamiltonian; i.e., their contributions to the rotational energy levels have almost identical effects. This large interdependence can be seen quantitatively in the correlation coefficient (*21*, Section D-2-c), $C(\gamma, A_D)$. For the First Negative bands, the $C(\gamma, A_D)$ coefficients were the largest ones in the array. For example $C(\gamma, A_D) = 0.991$ for the (3, 1) band. For molecular constants of such small magnitudes, this high correlation means that if one of these constants is omitted from the fit, the other can almost completely absorb the effect of its absence, i.e., the fitted values of all of the other constants and the standard deviation of the residuals are essentially unchanged. In absorbing the effect of the missing constant, the remaining member of the pair no longer, of course, represents the intended molecular interaction, but rather some blend of the two. Thus, if the reported values of A_D'' or γ'' are to be the best estimates of the strengths of their respective interactions, then *both* constants must be included simultaneously in the fit. Coxon (*24*), in his study of the OD $A^2\Sigma^+$–$X^2\Pi$ bands, has also discussed this point. Here, we test whether both A_D'' and γ'' should simultaneously be included or should simultaneously be omitted from the set of molecular constants. Table V shows that the F_e values are all much larger than the critical value of $F = 3.0$; hence, this *pair* of constants can be said to be nonzero with very high confidence.

Finally, Table V gives the F-tests for the Λ-doubling parameters q'' and p'', which are also best treated as a pair, since they both arise from the same interaction. From the magnitude of the F_e values, it is clear that these constants are required in the Hamiltonian. In these least-squares fits, we have assumed that the $a^4\Pi_u$ state is Λ doubled by a single $^4\Sigma_u$ state (*9*) and that this is a $^4\Sigma_u^+$ state that lies above the $a^4\Pi_u$ state. The reasons for the last two choices are the following. First, no $^4\Sigma$ states are theoretically expected to lie below the $a^4\Pi_u$ state (*25*). Secondly, when attempts are made to fit the data at hand with a $^4\Sigma_u^-$ state (above) as the single perturber of the $a^4\Pi_u$ state, the iterative nonlinear least-squares program attempts to change the sign of the q'' value, indicating that the minimum-variance fit to the data with a $^4\Sigma_u^-$ state requires that this state lie below the $a^4\Pi_u$ state. Consequently, only a perturbing $^4\Sigma_u^+$ state above the $a^4\Pi_u$ state is consistent with the present data and current theoretical considerations (*25*). All of the separately fit bands were consistent in this requirement.

The F-tests in Table V show that one could be very confident that the first 16 molecular constants given at the beginning of this section were significant for the present high-resolution data and that the need for any others was very small for the data set at hand. After the H_v' and H_v'' were omitted from the Hamiltonians and the bands refitted, the conclusions about the significance of γ', A_D'', and γ'', and q'' and p'' remain unchanged; namely, the new F_e values are very similar to those in Table V, as expected.[6]

[6] It is interesting to note that one does not actually have to refit with the tested constant(s) omitted. Hamilton (*20*, pp. 137–139) shows that the new constants and their variance–covariance matrix can be calculated from the results of the fit that includes the constants in question. This fact is at the heart of the F-test, as applied here.

TABLE VI. F-TESTS OF THE MOLECULAR CONSTANTS γ', A_D'', γ'', q'', p'', D', AND D'' FOR THE MODERATE-RESOLUTION FIRST NEGATIVE O_2^+ BANDS[a]

band[b]	degrees of freedom	$\gamma'(10^{-4})$	$F_e(\gamma')$	$A_D''(10^{-4})$	$\gamma''(10^{-3})$	$F_e(A_D'', \gamma'')$	$q''(10^{-5})$	$p''(10^{-3})$	$F_e(q'', p'')$	$F_e(D', D'')$
(0, 3)W	188	− 6.9(11.0)	0.397	− 1.8(5.0)	2.3(12.0)	0.819	− 6(15)	4.0(1.3)	4.88	68.6
(0, 4)W	169	−21.0(16.0)	1.68	12 (10)	− 29(23)	0.930	−20(31)	10.0 (3.2)	5.07	8.45
(0, 5)W	93	− 8.6(25.0)	0.116	0.9(8.7)	− 4 (22)	0.128	≈0(150)	4.1 (4.0)	1.47	57.7
(1, 4)W	209	− 6.3(20.0)	0.100	0.5(11.0)	− 4 (28)	0.415	≈0(37)	3.9 (2.9)	0.915	11.2
(1, 5)W	201	− 6.1 (13.0)	0.233	0.5 (6.8)	− 5 (17)	1.33	≈0(14)	4.1 (1.7)	3.15	47.6
(1, 6)W	112	29.0(34.0)	0.737	0.9 (14.1)	−185(27)	30.4	−14(53)	19.7 (4.5)	13.0	3.39

[a] See footnote a of Table V.

[b] W = Weniger (7)

The six bands of Weniger (7) were fitted with the 16 molecular constants that were found significant for the high-resolution data (H_v cannot be significant here). The results of the F-tests are given in Table VI. Recalling that the critical value of F_e is 3.9 for one constant and 3.0 for two constants, one can see that γ' and the pair A_D'' and γ'' do not appear to be significant for these data and are omitted. The unusually large $F_e(A_D'', \gamma'')$ value for the (1, 6) band is considered to be an anomaly. The constants q'' and p'' appear to be slightly needed and are retained. Finally, the constants D' and D'' are distinctly necessary. Therefore, the moderate-resolution bands were refit to 13 adjustable molecular constants.

b. Test for Normality

In addition to the assumptions (*21*, Section C-2) necessary for the validity of least-squares as a method of estimation of molecular constants (which are implicitly evoked here), the F-tests require the assumption that the measurement errors are normally distributed. Thus, a normality test is always appropriate in such cases. The residuals of the fit to the (3, 1) First Negative band were used as an example for one kind of normality test in Ref. (*21*, Fig. 10), where it is shown that the measurement errors are very nearly normally distributed. Similar results were found for Nevin's (*4, 5*), Nevin and Murphy's (*6*), and Weniger's (*7*) data, although to a much less extent for the last of these three.

RESULTS

Individual Band Fits

Table VII lists the values obtained for the molecular constants from nonlinear least-squares fits to each of the First Negative bands separately. The table groups the $b^4\Sigma_g^-$ and $a^4\Pi_u$ constants separately and, within each group, the bands are arranged to facilitate the comparison of the values obtained for the same vibrational level. One can see that most of the multiple values for the same constant agree very well in comparison to two or three times their standard errors. For example, the largest difference between the five B_0'' values is 0.00050 cm^{-1}, which is only two times the sum of the standard errors. Furthermore, many of the constants obtained from the moderate-resolution bands are in good agreement with those from the high-resolution bands. For example,

TABLE VII. THE MOLECULAR CONSTANTS OBTAINED FROM SEPARATE FITS TO THE INDIVIDUAL O_2^+ FIRST NEGATIVE BANDS.[a]

band[b]	degrees of freedom	σ	ν_0	B'	D' (10^{-6})	γ' (10^{-4})	ϵ'
(3, 1) P	316	0.0316	19037.530(7)	1.209462(110)	6.458(82)	−9.5(1.8)	0.1432(12)
(2, 0) P	181	0.0303	18958.127(6)	1.232030(130)	6.287(99)	−5.5(2.3)	0.1441(15)
(2, 0) N	211	0.0377	18958.168(9)	1.231924(150)	6.255(0.107)	−10.3(2.9)	0.1456(17)
(1, 6) W	115	0.28	12052.271(84)	1.26173(189)	7.5(3.1)	—	0.1717(178)
(1, 5) W	204	0.18	12962.886(29)	1.25325(68)	4.77(0.62)	—	0.1591(87)
(1, 4) W	212	0.28	13894.579(53)	1.25278(120)	4.9(1.2)	—	0.1431(130)
(1, 0) P	330	0.0245	17829.716(4)	1.254514(72)	6.195(43)	−5.6(1.2)	0.14486(91)
(1, 0) N[c]	301	0.0355	17829.705(7)	1.254886(106)	6.528(59)	−6.2(1.9)	0.1456(14)
(0, 5) W	96	0.15	11800.260(43)	1.27792(81)	8.31(0.86)	—	0.1541(120)
(0, 4) W	172	0.20	12731.669(46)	1.27555(95)	5.1(1.2)	—	0.1392(99)
(0, 3) W	191	0.11	13684.354(21)	1.27731(54)	6.40(0.60)	—	0.1607(55)
(0, 3) NM	287	0.0280	13684.433(6)	1.276727(86)	6.195(60)	−5.6(1.5)	0.1450(11)
(0, 2) N	340	0.0317	14657.980(5)	1.276639(84)	6.114(41)	−6.2(1.6)	0.1458(12)
(0, 1) N	291	0.0319	15652.188(6)	1.276634(100)	6.123(50)	−6.9(1.7)	0.1445(13)
(0, 0) N	278	0.0301	16667.025(6)	1.276888(95)	6.202(59)	−2.0(1.5)	0.1462(12)

[a] All units are reciprocal centimeters. The number in parentheses corresponds to one standard error expressed in terms of the last digits, i.e. 1.20946(11) is 1.20946 ± 0.00011.

[b] N = Nevin (4, 5), NM = Nevin and Murphy (6), W = Weniger (7), and P = present study.

[c] As explained in the text, this band was not included in the merged fit.

the three values for B_0' from the (0, 3), (0, 4), and (0, 5) bands of Weniger (7), while much less precise, agree with the high-resolution values within 0.00129 cm^{-1}, which is about two standard errors of the former. Other such favorable comparisons are encouraging indications that seriously debilitating systematic differences, even between different investigations, are probably absent.

However, Table VII is not completely free from troublesome differences. Two of the ϵ_1' values of Weniger seem a bit too different, as do the A_3'' values of Nevin and Murphy (6) and Weniger (7). However, this is not totally unexpected because of the systematic problems that could arise from the blending in the moderate-resolution data. However, the most serious, as well as inexplicable, anomalies in Table VII are the D_1' and D_0'' values from the (1, 0) band of Nevin (4). Both are *distinctly* larger than the other values for these constants, much more than what can reasonably be expected on the basis of the standard errors alone. It is probably no coincidence that the B_1' and B_0'' values from this same band are also the highest values for these constants. The correlation coefficients between B', D', B'', and D'' are all large and positive (from 0.778 to 0.987); hence, the errors in these constants tend to be of the same sign. The residuals of the fit to Nevin's (1, 0) data were carefully examined, but they gave no indication as to the source of this problem. However, the constant D_v is extremely sensitive to very small effects and one could expect that the origin of such a difference would be difficult to find. The (1, 0) band was photographed in the present study and the molecular constants show no such anomalous behavior, as can be seen in Table VII. This is fortunate, because as Fig. 1 shows, the (1, 0) band provides the *only* high-resolution link to the (1, 4), (1, 5), and (1, 6) moderate-resolution bands of Weniger, which, as will

TABLE VII. CONTINUED

band[a]	A''	$A_D''(10^{-4})$	B''	$D''(10^{-6})$	$\gamma''(10^{-3})$	ϵ''	$q''(10^{-5})$	$p''(10^{-3})$	α''
(1,6)W	−47.621(27)	–	1.01081(180)	6.5(2.8)	–	0.5744(160)	−109(52)	12.9(4.4)	0.284(58)
(1,5)W	−47.626(14)	–	1.01812(70)	3.91(0.62)	–	0.6369(75)	≈0 (14)	3.9(1.2)	0.222(17)
(0,5)W	−47.636(23)	–	1.02048(89)	7.5(1.0)	–	0.6519(89)	≈0 (30)	3.9(2.0)	0.145(28)
(1,4)W	−47.757(22)	–	1.03344(120)	4.2(1.2)	–	0.6312(109)	≈0 (34)	3.9(2.6)	0.204(35)
(0,4)W	−47.771(17)	–	1.03404(93)	4.9(1.3)	–	0.6265(80)	−5 (27)	8.7(2.4)	0.196(25)
(0,3)W	−47.7964(83)	–	1.05120(56)	5.70(0.60)	–	0.6150(45)	−5 (15)	4.6(1.1)	0.194(13)
(0,3)NM	−47.7478(35)	0.24(0.74)	1.050609(96)	5.245(58)	−3.3(1.7)	0.6201(15)	−1.1(1.7)	4.01(0.18)	0.1755(23)
(0,2)N	−47.7800(36)	0.46(0.64)	1.066045(86)	5.132(41)	−4.1(1.5)	0.6138(14)	−0.4(1.1)	4.19(0.16)	0.1564(23)
(3,1)P	−47.8031(39)	−1.86(0.92)	1.081646(110)	5.111(82)	0.9(2.1)	0.6125(16)	−3.8(2.4)	3.49(0.24)	0.13 0(28)
(0,1)N	−47.7859(40)	1.14(0.77)	1.081513(100)	5.116(55)	−6.4(1.8)	0.6162(16)	−1.9(1.4)	3.70(0.17)	0.1357(28)
(2,0)P	−47.7875(53)	0.4(1.2)	1.096983(140)	5.041(0.100)	−4.6(2.9)	0.6090(22)	−0.6(3.0)	3.96(0.28)	0.1242(34)
(2,0)N	−47.7874(60)	1.8(1.4)	1.096942(160)	5.036(0.110)	−8.0(3.3)	0.6079(25)	−6.5(3.3)	3.68(0.34)	0.1271(40)
(1,0)P	−47.7931(27)	0.91(0.61)	1.097050(73)	5.067(43)	−5.5(1.4)	0.6129(16)	−1.2(1.1)	3.91(0.15)	0.1216(20)
(1,0)N[c]	−47.8093(40)	−0.01(0.90)	1.097443(108)	5.417(60)	−3.1(2.0)	0.6090(18)	−1.8(1.5)	3.70(0.22)	0.1246(32)
(0,0)N	−47.7938(37)	1.28(0.79)	1.097215(95)	5.171(56)	−5.8(1.8)	0.6126(15)	−3.2(1.6)	3.97(0.18)	0.1202(26)

be noted below, is the key to improved values for the molecular constants of the $v'' = 4$, 5, and 6 levels of the $a^4\Pi_u$ state. After omitting the (1, 0) of Nevin, the remaining values in Table VII show fairly good internal consistency.

Merged Fit

Table VII does not contain the best *single* values for the molecular constants of each vibrational level. For example, there are four high-resolution bands that yield separate values for B_0' and five that yield values for B_0'', thereby presenting the opportunity for substantial statistical gains in precision by combining these data.

One approach that would take advantage of multiple bands associated with many of the vibrational levels is to make *one* weighted least-squares fit to the data of all of the bands simultaneously, using weights based on the standard deviations in Table VII, to determine the best *single* values for the molecular constants of the vibrational levels involved. While very appealing in simplicity, this approach would require an iterative nonlinear least-squares fit of 83 molecular constants to over 3500 measurements, a formidably time consuming and expensive computing task. One naturally looks for better ways to accomplish the same statistical gain.

In an accompanying paper (*26*), we describe a fairly simple method for doing this. Briefly, it uses the sets of molecular constants from the 14 individually fitted bands given in Table VII (where the (1, 0) band of Nevin (*4*) is excluded) and the accompanying variance–covariance matrices as input to a *linear correlated* least-squares fit to determine the best set of single values for the molecular constants and their standard errors for each vibrational level involved. The details are given in Ref. (*26*) and it only need be mentioned here that such a correlated fit properly takes into account all of the features of the results of Table VII, i.e., the different standard errors of the multiple values for each constant and the correlation between the errors of the constants in each band. The fitted constants are *exactly* the same values that would be obtained from

TABLE VIII. MERGED MOLECULAR CONSTANTS OF THE O_2^+ $b^4\Sigma_g^-$ AND $a^4\Pi_u$ STATES.[a]

	v'	T'	B'	$D'(10^{-6})$	$\gamma'(10^{-4})$	ϵ'
$b^4\Sigma_g^-$	3	20052.379(13)	1.209440(80)	6.478(65)	−9.6(2.1)	0.1433(23)
	2	18958.145(8)	1.232069(73)	6.336(49)	−6.6(1.9)	0.1449(22)
	1	17829.716(7)	1.254512(68)	6.233(41)	−6.0(1.5)	0.1451(17)
	0	16667.025(8)	1.276727(66)	6.133(40)	−4.9(1.2)	0.1454(11)

95 degrees of freedom
$\sigma_M = 1.95$

	v''	T''	A''	$A_D''(10^{-4})$	B''	$D''(10^{-6})$	$\gamma''(10^{-3})$	ϵ''	$q''(10^{-5})$	$p''(10^{-3})$	α''
$a^4\Pi_u$	6	5777.401(0.16)	−47.581(52)	—	1.00452(87)	5.34(0.84)	—	0.585(29)	−183(100)	11.6(7.9)	0.199(0.101)
	5	4866.798(44)	−47.635(19)	—	1.01930(22)	5.25(0.20)	—	0.640(10)	−1(24)	3.1(1.9)	0.189(28)
	4	3935.283(64)	−47.777(26)	—	1.03491(32)	5.39(0.36)	—	0.633(12)	2(40)	6.0(3.3)	0.188(37)
	3	2982.609(13)	−47.758(59)	−1.6(1.2)	1.050597(72)	5.178(42)	1.3(2.9)	0.6172(26)	−0.7(3.2)	4.19(0.34)	0.1773(45)
	2	2009.046(13)	−47.780(69)	0.4(1.2)	1.066132(70)	5.151(41)	−3.8(2.9)	0.6138(28)	−0.4(2.2)	4.20(0.32)	0.1565(45)
	1	1014.842(13)	−47.795(51)	−0.1(1.1)	1.081611(68)	5.125(42)	−3.3(2.6)	0.6144(21)	−2.5(2.4)	3.65(0.27)	0.1372(37)
	0	≡0	−47.791(36)	1.05(0.82)	1.097050(67)	5.104(39)	−5.8(1.9)	0.6114(15)	−2.2(1.6)	3.91(0.20)	0.1227(26)

[a] See footnote a of Table VII.

the massive, weighted fit to all of the measured line positions directly that was mentioned above, if it were practical. Furthermore, because of the relatively large degrees of freedom in the fit to each band (Table VII), the standard errors of the molecular constants are expected to have their usual statistical meaning in regard to constructing the familiar confidence limits (*26*).

Table VIII contains the results of merging the 178 partially redundant molecular constants in Table VII into 83 constants, one value of each type of constant for each vibrational level.[7] There are improvements of several types. Some of the gain is clearly just the familiar increase in precision that accompanies an increase of data. For example, the merged value for B_0'' of 1.097050(67) cm^{-1} is more precise than any of the multiple values in Table VII. Other improvements occur due to the "propagation of precision" through large covariances (i.e., high correlation).

For example, even though the $v' = 3$ vibrational level has only single values for the molecular constants in Table VII, the new merged value for B_3' is different and more precise, 1.209440(80) cm^{-1}. The reason is that when the best single value of B_1'' is established in the merged fit, the strong correlation between B_3' and B_1'' in the (3, 1) band forces B_3' to assume a new value and the precision of B_1' is somewhat "propagated" via the more accurate $\Delta B \equiv B_3' - B_1''$ into B_3'. A similar, but more dramatic improvement, occurs for the merged values associated with vibrational levels $v'' = 4$, 5, and 6 for which there are only moderate-resolution measurements. For example, the merged value for B_6'' is 1.00452(87) cm^{-1}, which is a factor of two more precise than the value in Table VII for the (1, 6) band, reflecting the propagation of *part* of the precision of the B_1' value. In fact, the standard error of B_6'', 8.7×10^{-4} cm^{-1}, has been reduced to essentially that of $\Delta B \equiv B_1' - B_6''$ in the fit to the (*1*, 6) band, below which it cannot be further reduced without the *additional* benefit of multiple values. Lastly, it should be noted that the moderate-resolution data do little to improve the precision of the constants of levels that already are involved in the high-resolution data. This is due, of course to there being factors of 4 to 150 differences in the precision of the values of the two data sets; thus, the interrelations imposed on the whole set by the moderate-

[7] The zero of the term energy is referenced to the unsplit, nonrotating H_0 of the $v'' = 0$ level, as defined by Eqs. (1) and (2).

precision data are relatively weak. In summary, Table VIII contains the minimum-variance values for the constants of each vibrational level that are consistent with *all* of the multiple values *and* their variances (standard errors) and interrelating covariances (correlations).

Reference (*26*) shows that the size of the variance of the residuals of the merge fit, σ_M^2, is a convenient indicator of the internal consistency of the values being merged. For the 95 degrees of freedom of this fit, it is expected that the variance σ_M^2 would lie between the limits 0.74 and 1.31 with 0.95 probability if all of the measurement errors are randomly (and normally) distributed. The value $\sigma_M^2 = 3.81$ obtained in the present fit lies distinctly outside of these limits; thus, we must accept the strong possibility that relative systematic errors are present to some extent in this set of First Negative data. From the studies in Ref. (*26*), however, it appears that these errors may not be excessively large, perhaps about twice as large as the random errors. Otherwise σ_M^2 would have been very large indeed (and the inconsistencies in Table VII would have been quite apparent to visual inspection).

The test cannot, unfortunately, identify the offending data, since only *relative* errors are detected. Because of the large number of unresolved blends and the systematic problems that this can cause, one suspects that the bulk of the problem may lie with the moderate-resolution data (*7*). However, a merged fit to only the eight high-resolution bands suggests that they are not entirely free from problems either. The 53-degrees-of-freedom fit yields $\sigma_M^2 = 2.54$, which is outside of the 0.66 and 1.42 limits of 0.95 probability.

In view of this strong possibility that the relative systematic errors may be as large as, or even slightly larger than, the random measurement errors, one must exercise extra caution in constructing confidence limits for the molecular constants in Table VIII from the values and standard errors given there. The limited systematic error studies in Ref. (*26*) suggest that, since σ_M^2 (and hence the standard errors) have increased *because* of these relative systematic errors, the larger confidence limits constructed from the standard errors in the usual way (*21*, Section D-3-b) stand the implied chance of including the unknown "true" molecular constants, in spite of the relative systematic errors. Nevertheless, caution dictates that we recommend about three standard errors (rather than the two that would be called for in the case of purely random errors) in the construction of $\approx 95\%$ confidence limits for the constants in Table VIII.

Dunham Coefficients

The values in Table VIII correspond to the adjustable constants in the model Hamiltonians discussed above. The merged fit imposed no additonal physics. However, it is useful to merge the results of the band-by-band fits (Table VII) by imposing the familiar rovibronic Dunham model (*27*):

$$\nu_0(v', v'') = T_e + \sum_{i=1} Y_{i0}'(v' + \tfrac{1}{2})^i - \sum_{j=1} Y_{j0}''(v'' + \tfrac{1}{2})^j, \tag{13}$$

$$B_v = \sum_{i=0} Y_{i1}(v + \tfrac{1}{2})^i, \tag{14}$$

and

$$D_v = \sum_{i=0} Y_{i2}(v + \tfrac{1}{2})^i. \tag{15}$$

Purely for the purpose of extending this convenient summarization of data, we also include the ad hoc expansions

$$(\gamma_v, \epsilon_v, A_v, A_{Dv}, q_v, p_v, \text{ or } \alpha_v) = \sum_{i=0} Y_{Xi}(v + \tfrac{1}{2})^i, \tag{16}$$

where X may stand for any of the indicated seven "magnetic" constants.

In fitting this model to the data in Table VII, one must choose the proper termination order of 14 polynomials. Several of these are obvious; e.g., only the first member of the polynomial is required for A_D'', q'', and p'', in view of the lack of v variation relative to about two standard errors in Table VIII. Others are not so obvious. As a first guide, we used a mixed model in the merged fit to determine one Y polynomial at a time and v-dependent molecular constants (like in Table VIII) for the remainder of the model. The order of the polynomial series in each fit was determined in a standard statistical way (*20*). Finally, we made merge fits with the whole Y model, varying the order of the few less well determined polynomials (e.g., $Y_{\gamma i}''$) in succession to select the best final orders for a simultaneous fit. Table IX contains these polynomial coefficients. Because of the high correlation (≥ 0.95) that exists between many of the polynomial coefficients, the values in Table IX were checked by back calculation to be sure that their relative precision had been preserved in rounding to the digits given (*21*, Section G-1-d).

Thus, as an alternative to the 80 molecular constants in Table VIII, the First Negative data are also represented by the 32 polynomial coefficients of Table IX. The fit to the data probably has deteriorated a little by imposing the Dunham model; σ_M increased from 1.95 to 2.36 cm^{-1}, which is an increase of about three standard errors (0.14 cm^{-1}) of σ_M of Table VIII (*21*, Section G-1-e). However, the polynomial coefficients in Table IX and the Dunham model now permit extrapolation to higher vibrational levels of both electronic states, a useful feature, and something the molecular constants of Table VIII cannot do. Thus, for the prediction of line positions of bands with $0 \leq v' \leq 3$ and $0 \leq v'' \leq 6$, the constants of Table VIII are preferred and for bands with $v' > 3$

TABLE IX. DUNHAM COEFFICIENTS FOR THE $b^4\Sigma_g^-$ AND $a^4\Pi_u$ STATES OF O_2^+ [a]

		1	$v+\frac{1}{2}$	$(v+\frac{1}{2})^2$	$(v+\frac{1}{2})^3$
$b^4\Sigma_g^-$ $0 \leq v \leq 3$	$G(v)$	$T_e = 16587.867(20)$	1197.0225(288)	−17.1787(160)	$9.617(2.680)\times10^{-3}$
	B_v	1.28774 53(820)	$-2.98372(344)\times10^{-2}$	$-1.1211(723)\times10^{-4}$	
	D_v	$6.0750(477)\times10^{-6}$	$1.074(0.135)\times10^{-7}$		
	γ_v	$-4.330(1.590)\times10^{-4}$	$-1.183(0.664)\times10^{-4}$		
	ϵ_v	0.14499(99)			
$a^4\Pi_u$ $0 \leq v \leq 6$	$G(v)$	$T_e = 0$	1035.2272(172)	−10.16526(657)	$-2.6148(737)\times10^{-2}$
	A_v	−47.78561(539)	$-1.868(0.585)\times10^{-2}$	$7.967(1.280)\times10^{-3}$	
	A_{Dv}	$4.65(6.18)\times10^{-5}$			
	B_v	1.1047456(814)	$-1.53730(217)\times10^{-2}$	$-2.860(0.408)\times10^{-5}$	
	D_v	$5.0937(464)\times10^{-6}$	$2.235(0.767)\times10^{-8}$	146 degrees of freedom	
	γ_v	$-4.662(1.420)\times10^{-3}$	$2.970(1.140)\times10^{-4}$	$\sigma_M = 2.36$	
	ϵ_v	0.60889(167)	$3.253(0.767)\times10^{-3}$		
	q_v	$-1.73(1.27)\times10^{-5}$			
	p_v	$3.961(0.156)\times10^{-3}$			
	α_v	0.11446(312)	$1.687(0.153)\times10^{-2}$		

[a] See footnote a of Table VII.

and/or $v'' > 6$, the constants given by the coefficients in Table IX must be used (and with discretion, when $v' \gg 3$ and $v'' \gg 6$).

The single coefficient for A_{Dv} in Table IX is very poorly determined and it is not worthwhile to compare it to the harmonic approximations for A_{Dv} derived by Veseth (*28*) and Merer (*29*). The latter do predict that it will be exceedingly difficult to determine a significant A_{Dv} value for the O_2^+ $a^4\Pi_u$ state because its magnitude is proportional to the v variation of A_v. The three Y_{Ai} coefficients in Table IX yield fitted A_v values whose "v derivative" changes sign between $v = 0$ and $v = 2$, thus predicting a near-zero value for A_{Dv} in this region. The only statement that the present data can make is that $-1.4 \times 10^{-4} \leq A_{Dv} \leq 2.3 \times 10^{-4}$ cm^{-1} with roughly 0.95 probability. If A_{Dv} had been omitted from the $^4\Pi_u$ Hamiltonian, however, the values obtained for γ'' would have been about a factor of two smaller, having been forced to represent two different constants. One could fix the A_{Dv} constant in the fits to the value given by the harmonic approximation, but without a test of the degree of applicability of these models to the $a^4\Pi_u$ state, this seems unwarranted. Furthermore, the implicit assumption of no error in the fixed values would produce erroneously optimistic uncertainties on the resulting values for γ_v''. We think that the values in Tables VIII and IX represent the best estimates, even though they are relatively poor ones, of the constants representing the two *separate* molecular interactions.

Theoretical D_v Values

Another model that could be imposed on the data is the assumption that the mechanical rotation contribution to the two-dimensional potential is proportional to $J(J+1)/r^2$, where r is the internuclear separation. This permits rotational centrifugal distortion constants to be calculated via perturbation techniques from the *rotationless* potential, which is specified by the $G(v)$ and B_v values (*30*). If the calculated D_v values are consistent with the experimental values (i.e., if the latter scatter about the former within the experimental uncertainties), then one is justified in imposing this additional

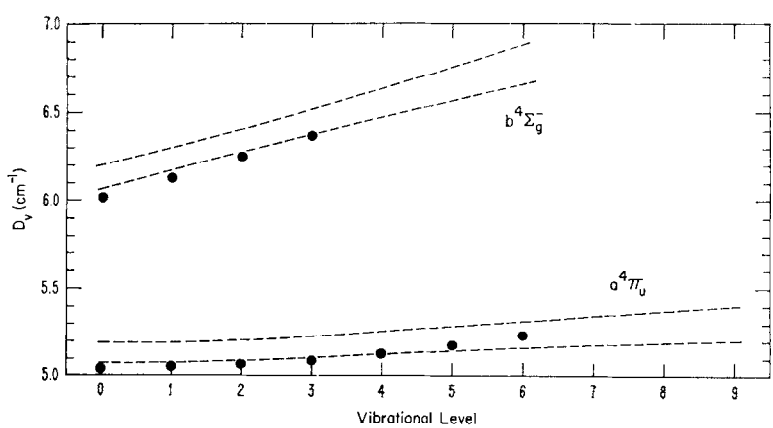

FIG. 5. D_v values for the O_2^+ $b^4\Sigma_g^-$ and $a^4\Pi_u$ states. The circles are values calculated from *RKR* potentials. The pairs of dashed lines enclose a ± 3 standard error region given by the D_v polynomial coefficients in Table VIII and their variance–covariance matrix.

model on the data and can fix the D_v values in the fit to the calculated values. This generally improves the precision of the fitted B_v values, and the process can be iterated, if necessary, to obtain a set of fitted $\nu_0(v', v'')$ and B_v values and calculated D_v values that are consistent with the $J(J+1)/r^2$ model. References (*31*) and (*32*) give examples of this application.

For the present data, *RKR* potentials were constructed from the coefficients in Table IX, and D_v' and D_v'' values were calculated from them. These values are denoted by the circles in Fig. 5. Each pair of dashed lines enclose the ± 3 standard error region calculated from the D_v polynomial coefficients and their variance–covariance matrix, (*21*, Section G-2-a). Only a few of the calculated values lie inside of this region. As a check, we also calculated D_v and H_v values from potentials based on Y_{ij} values from least-squares fits in which H_v *was* included in the Hamiltonians. The comparison between calculated and fitted values was still not satisfactory. Hence, we have not felt fully justified in applying this method to the present data.

Possible Perturbation

In the reduction of the (0, 3) band of Nevin and Murphy (*6*) to molecular constants, it was found that the high J lines of several branches gave relatively large and systematic residuals in the least-squares fit. No combination of molecular constants could produce a satisfactory fit to these lines. However, when they were omitted from the fit, the remaining lines were fitted as well as those in the rest of Nevin's bands. The offending branches were Q_1 and ${}^QP_{21}$ for $J'' > 36\frac{1}{2}$ and P_4 and the blended pair ${}^PR_{24}$–${}^PQ_{34}$ (see Table I) for $J'' > 32\frac{1}{2}$. These four branches are among the strongest in the O_2^+ First Negative bands and thus could be followed to significantly higher rotational levels than the other bands. Consequently, combination differences involving these perturbed lines could *not* be formed. Nevin and Murphy employed the combination-difference method to reduce their data to molecular constants; hence, these lines were not used by them.

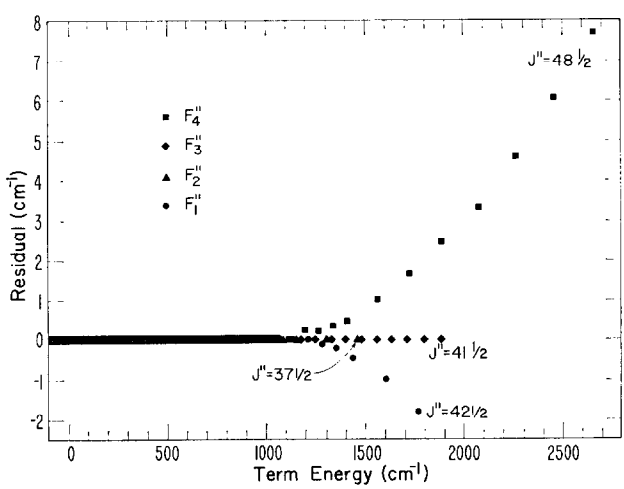

FIG. 6. Average residuals of the fit to the lines of the (0, 3) First Negative band grouped by F'' component and rotational term energy of the $v'' = 3$ level of the $a^4\Pi_u$ state. The zero of energy is referenced to the unsplit, nonrotating H_0 of the $v'' = 3$ level, as defined by Eqs. (1) and (2).

Perhaps this is why the anomaly went unnoticed in their investigation. Furthermore, Veseth (*17*) used the term value method (*33*) to obtain the molecular constants in his analysis of these data. This method requires that the rotational levels be interconnected (*34*); thus, these anomalous lines again could not be used and went unnoticed in that analysis also. In contrast to these two methods, the direct two-Hamiltonian fit (see footnote 1 of Ref. (*26*)) applied in the present study to each band *can* use such lines and thus their anomalous wavenumbers were noticed.

For the other $(0, v'')$ bands of this system with $v'' \neq 3$, these lines were fitted straightforwardly. Thus, Nevin and Murphy's data for the (0, 3) band (Weniger's less rotationally developed data for this band do not extend to these J levels) indicate that the F_1 and F_4 components of the $v = 3$ level of the $a^4\Pi_u$ state are possibly perturbed for $J > 36\frac{1}{2}$ and $J > 32\frac{1}{2}$, respectively. Figure 6 shows the anomaly more graphically. Below a $v'' = 3$ rotational term energy of about 1200 cm^{-1}, the residuals of the fit to the (0, 3) band that correspond to *all four* F'' components are typically 0.03 cm^{-1}. Above this energy, the residuals associated with *only* the F_2'' and F_3'' continue to show the same quality of fit. However, the residuals associated with the F_1'' and F_4'' components rapidly deviate in an opposite and systematic manner, which is characteristic of a perturbation.

We have, in fact, attempted to explain this behavior as a perturbation of the $a^4\Pi_u$ state by another electronic state, but without success. The requirements of a perturbation are that both states have the same ungerade symmetry and that the nearly coincident levels have the same rotational quantum numbers J. The nearest known candidate is the $A^2\Pi_u$ state, but its zeroth vibrational level lies about 3400 cm^{-1} above the site of this anomaly. The relative location of the doublet and quartet manifolds are based on accurate Rydberg-series (*35*), photoionization (*36*), and photoelectron (*37*) studies and thus this value of 3400 cm^{-1} cannot be significantly in error. The ab initio calculations of Beebe, Thulstrup, and Anderson (*25*) place all other ungerade state even higher. Thus, we are unable to attribute directly the anomalous behavior of $a^4\Pi_u$, $v = 3$, to a perturbation from another electronic state.

We have also considered that the anomaly arises from self-perturbation (*38*), i.e., an interaction between F components of different vibrational levels of the $a^4\Pi_u$ state. However, the relatively small spin–orbit splitting constant A_v'' rules out this possibility for the affected J'' values. Lastly, since these perturbed lines would be difficult to assign properly without combination differences available, we considered the possibility that they indeed belong to another First Negative band that lies under the (0, 3) band. This search also proved futile.

Without a direct examination of the plate(s) of the (0, 3) band, additional speculation seems unwarranted. We suggest that here is a problem meriting further spectroscopic study, particularly since the (0, 5) and (1, 5) bands recorded by Weniger (*7*) with only moderate resolution show anomalies that appear somewhat similar to the one discussed here.

ACKNOWLEDGMENTS

We wish to thank Dr. S. Weniger for sending us unpublished line positions and Dr. E. W. Thulstrup for sending the manuscript of Ref. (*25*) prior to its publication. One of us (R.N.Z.) gratefully acknowledges support from the National Science Foundation.

RECEIVED: January 24, 1977

REFERENCES

1. Y. Tanaka and T. Takamine, *Sci. Pap. Inst. Phys. Chem. Res. Tokyo* **39**, 437 (1942).
2. P. H. Krupenie, *J. Phys. Chem. Ref. Data* **1**, 423 (1972).
3. W. Lindinger, D. L. Albritton, M. McFarland, F. C. Fehsenfeld, A. L. Schmeltekopf, and E. E. Ferguson, *J. Chem. Phys.* **62**, 4101 (1975).
4. T. E. Nevin, *Philos. Trans. R. Soc. London Ser. A* **237**, 471 (1938).
5. T. E. Nevin, *Proc. R. Soc. London Ser. A* **174**, 371 (1940).
6. T. E. Nevin and T. Murphy, *Proc. R. Ir. Acad. Sect. A* **46**, 169 (1941).
7. S. Weniger, *J. Phys. Radium* **23**, 225 (1962).
8. F. C. Fehsenfeld, K. M. Evenson, and H. P. Broida, *Rev. Sci. Instrum.* **36**, 294 (1965).
9. R. N. Zare, A. L. Schmeltekopf, W. J. Harrop, and D. L. Albritton, *J. Mol. Spectrosc.* **46**, 37 (1973).
10. T. C. James, *J. Chem. Phys.* **41**, 631 (1964).
11. L. Veseth, *J. Phys. B* **3**, 1677 (1970).
12. A. Budó, *Z. Phys.* **105**, 73 (1937).
13. W. H. Brandt, *Phys. Rev.* **50**, 778 (1936).
14. A. Budó and I. Kovács, *Hung. Acta Phys.* **4**, 273 (1954).
15. I. Kovács, *Phys. Rev.* **128**, 663 (1962).
16. I. Kovács and S. Weniger, *J. Phys. Radium* **23**, 377 (1962).
17. L. Veseth, *Phys. Scr.* **12**, 125 (1975).
18. R. N. Zare, *in* "Molecular Spectroscopy: Modern Research" (K. Narahari Rao and C. W. Mathews, Eds.), Chap. 4.2, Academic Press, New York, 1972.
19. A. G. Worthing and J. Geffner, "Treatment of Experimental Data," p. 171, Wiley, New York, 1943.
20. W. C. Hamilton, "Statistics in Physical Science," pp. 139–142, 168–172, Ronald Press, New York, 1964.
21. D. L. Albritton, A. L. Schmeltekopf, and R. N. Zare, *in* "Molecular Spectroscopy: Modern Research" (K. Narahari Rao, Ed.), Vol. II, Chap. 1, Academic Press, New York, 1976.
22. G. Herzberg, "Spectra of Diatomic Molecules," pp. 109, 560, Van Nostrand, Princeton, N. J., 1950.
23. R. N. Zare, A. L. Schmeltekopf, D. L. Albritton, and W. J. Harrop, *J. Mol. Spectrosc.* **46**, 174 (1973).
24. J. A. Coxon, *J. Mol. Spectrosc.* **58**, 1 (1975).
25. N. H. F. Beebe, E. W. Thulstrup, and A. Andersen, *J. Chem. Phys.* **64**, 2080 (1976).
26. D. L. Albritton, A. L. Schmeltekopf, and R. N. Zare, *J. Mol. Spectrosc.* **67**, 132–156 (1977).
27. J. L. Dunham, *Phys. Rev.* **41**, 721 (1932).
28. L. Veseth, *J. Phys. B* **3**, 1677 (1970).
29. A. J. Merer, *Mol. Phys.* **23**, 309 (1972).
30. D. L. Albritton, W. J. Harrop, A. L. Schmeltekopf, and R. N. Zare, *J. Mol. Spectrosc.* **46**, 25 (1973).
31. D. L. Albritton, W. J. Harrop, A. L. Schmeltekopf, and R. N. Zare, *J. Mol. Spectrosc.* **46**, 89 (1973).
32. J. Wei and J. Tellinghuisen, *J. Mol. Spectrosc.* **50**, 317 (1974).
33. N. Åslund, *Ark. Fys.* **30**, 377 (1965).
34. D. L. Albritton, W. J. Harrop, A. L. Schmeltekopf, R. N. Zare, and E. L. Crow, *J. Mol. Spectrosc.* **46**, 67 (1973).
35. K. Yoshino and Y. Tanaka, *J. Chem. Phys.* **48**, 4859 (1968).
36. J. A. R. Samson and J. L. Gardner, *Can. J. Phys.* **53**, 1948 (1975).
37. O. Edqvist, E. Lindholm, L. S. Selin, and L. Åsbrink, *Phys. Scr.* **1**, 25 (1970).
38. A. Jenonvrier, B. Pascat, and H. Lefebvre-Brion, *J. Mol. Spectrosc.* **45**, 46 (1973).